

MET O 11 TECHNICAL NOTE NO. 154

A SUCCESSIVE CORRECTION ANALYSIS SCHEME USING RECURSIVE  
NUMERICAL FILTERS

by

R J PURSER and R McQUIGG

Meteorological Office (Met O 11)  
London Road  
Bracknell  
Berkshire  
United Kingdom

NB: This paper has not been published. Permission to quote from it must be obtained from the Assistant Director of the above Meteorological Branch.

March 1982

A SUCCESSIVE CORRECTION ANALYSIS SCHEME USING RECURSIVE NUMERICAL FILTERS

by

R J Purser and R McQuigg

ABSTRACT

An empirical objective analysis scheme is described based on the iterative method of successive correction. The scheme employs recursive numerical filters to disperse the observational information smoothly throughout the analysis grid. The chief merit of the scheme is its simplicity and versatility of use. Some mesoscale applications are demonstrated using conventional surface data.

## 1. INTRODUCTION

The successive correction technique for meteorological data analysis has been pioneered by Bergthorssen and D88s (1955), Cressman (1959) and others and applied successfully in a number of operational forecasting centres. More recently there has been a tendency to use methods more firmly based on rigorous statistical principles as in the case of optimal interpolation developed by Gandin (1963), Rutherford (1972), Bergman (1979) and Lorenc (1981), or else to use methods which also incorporate a numerical model in order to guide the analysis dynamically towards a state compatible with the model's own balance. These latter methods tend to be rather more expensive per analysis in terms of computer time. For many applications it is not actually necessary that analyses are optimal and accurately balanced, but rather that they are convenient and cheap to produce. From work that began as an attempt to investigate the feasibility of analysing mesoscale meteorological data in four dimensions a bi-product has been a suite of analysis programs that can be readily applied to subsynoptic rectangular areas for the analysis of conventional surface data. The technique is based on the multiple application of adaptive recursive averaging filters which ensure that the corrections indicated by the observation residuals are smooth. In this note a description is given of the strategy used for analysing data and examples of the applications of the scheme are presented.

## 2. RECURSIVE FILTERS

The numerical basis of the analysis method is the recursive filter which is used to produce a smooth local weighted average of the input field. The type of filter used is exemplified by the following simple one-dimensional version of the algorithm in which A is the input field and B is the smoothed output:

$$\left. \begin{aligned} B_0 &= A_0 \\ B_n &= \alpha B_{n-1} + (1-\alpha) A_n \quad n > 0 \end{aligned} \right\} \quad (1)$$

The smoothing parameter,  $\alpha$ , lies between 0 and 1. When  $n$  is sufficiently large for the boundary at  $n = 0$  to be ignored then we may expand the recursion in (1) and write  $B$  as the series:

$$B_n = (1-\alpha)(A_n + \alpha A_{n-1} + \alpha^2 A_{n-2} + \dots + \alpha^m A_{n-m} \dots) \quad (2)$$

Writing,

$$\begin{aligned} E_n &= (1-\alpha)\alpha^n & n \geq 0 \\ &= 0 & n < 0 \end{aligned} \quad (3)$$

then the convolution (2) can be expressed symbolically:

$$B = E * A \quad (2')$$

There are a number of features concerning the basic filter that are worth noting. Firstly it has an unbounded range in the sense that all  $A_m$  with  $m \leq n$  have an influence on the value of  $B_n$ . This enables the filter to carry information input from  $A$  across the entire grid in a single sweep. The characteristic response (ie a decaying exponential) retains the same shape for all permitted values of  $\alpha$  so the effect of a particular filter (or a combination of filters) can be easily reproduced on a different size grid with a correspondingly adjusted  $\alpha$ . In fact there is a normalised continuous analogue to any basic filter used consisting of the continuous convolution,

$$B(x) = -\log \alpha \int_0^{\infty} A(x-x') \alpha^{x'} dx' \quad (4)$$

which becomes an increasingly plausible approximation as  $\alpha \rightarrow 1$ . Another important property of the filter is that its effective smoothing range, given by the standard deviation of the convolution kernel,  $E$ , can take any positive magnitude according to the value of  $\alpha$ . We shall always regard (4) as a sufficiently good approximation to the discrete filters used when discussing theoretical aspects of them. Thus we may approximate the first and second moments of the distribution (3) with those of (4):

$$\begin{aligned}
 M_1 &= \sum_{n=0}^{\infty} n(1-\alpha)\alpha^n = \frac{\alpha}{(1-\alpha)} \simeq \lambda \\
 M_2 &= \sum_{n=0}^{\infty} n^2(1-\alpha)\alpha^n = \frac{\alpha(1+\alpha)}{(1-\alpha)^2} \simeq 2\lambda^2
 \end{aligned}
 \tag{5}$$

where  $\lambda = -\frac{1}{\log \alpha}$

A measure of the spread of the convolution is the variance of  $E$  about its mean:

$$M_2' = M_2 - M_1^2 = \frac{\alpha}{(1-\alpha)^2} \simeq \lambda^2
 \tag{6}$$

Thus  $\lambda$  may be regarded as an approximation to the characteristic smoothing range of this basic filter.

Under the successive application of normalised (ie  $M_0 = 1$ ) smoothing filters the quantities,  $M_1$  and  $M_2'$ , behave additively. It is easier to understand the effect of several applications by inspecting the Fourier representations of the fields involved. We define the Fourier transform conventions for one-dimension:

$$\begin{aligned}
 A_n &= \frac{1}{2\pi} \int_{-\pi}^{\pi} \tilde{A}(k) e^{ikn} dk \\
 \tilde{A}(k) &= \sum_{n=-\infty}^{\infty} A_n e^{-ikn} \\
 \text{or } \tilde{A}(k) &= \int_{-\infty}^{\infty} A(x) e^{-ikx} dx
 \end{aligned}
 \tag{7}$$

and also the convolution theorem:

$$B = E * A \iff \tilde{B} = \tilde{E} \tilde{A} \tag{8}$$

The transform of the basic filter function becomes:

$$\tilde{E}(k) = (1-\alpha) \sum_{n=0}^{\infty} (\alpha e^{-ik})^n$$

ie

$$\tilde{E}(k) = \frac{(1-\alpha)}{(1-\alpha e^{-ik})} \approx \frac{1}{(1+i\lambda k)} \tag{9}$$

Where again we have included the approximation appropriate to (4) which is valid for  $\lambda k \ll 1$ .

By the convolution theorem the effect of the application of filter,  $\tilde{E}$ , followed by its conjugate,  $\tilde{E}^+$ , acting in the opposite direction, is given in spectral form by the response function:

$$\tilde{S} = \widetilde{(E * E^+)} = \tilde{E}(k) \tilde{E}^*(k)$$

$$\text{ie } \tilde{S}(k) = \frac{1}{\left(1 + \frac{\alpha}{(1-\alpha)^2} \left(2 \sin \frac{k}{2}\right)^2\right)} \quad (10)$$

The corresponding analogue approximation gives:

$$\tilde{S}(k) \approx \frac{1}{(1 + \lambda^2 k^2)} = \frac{1}{2} (\tilde{E} + \tilde{E}^*) \quad (11)$$

The function,  $S$ , is in each case a symmetric pair of back-to-back decreasing exponentials. When the discretisation error is small enough to ignore we notice that successive applications of these filters necessarily leads to increasing smoothness as determined by the minimum order discontinuities in the field of smoothed values. (A zeroth order discontinuity is a discontinuity of the function itself, a first order discontinuity is a discontinuity in the first derivative, and so on). Nth order discontinuities in A result in a contribution to  $\tilde{A}(k)$  with asymptotic rate of decrease of order,  $\left| \frac{1}{k^{(n+1)}} \right|$  for large  $k$ . Thus each application of either  $E$  or  $E^+$  increases the order of any discontinuity by one.

The repeated application of continuous filter,  $S$ ,  $L$  times results in the spectral response:

$$\tilde{S}^L(k) = \frac{1}{(1 + \lambda^2 k^2)^L} \quad (12)$$

Which for sufficiently large  $L$  or small  $\lambda k$  is approximately:

$$\left. \begin{aligned} \tilde{S}^L(k) &\approx e^{-L\lambda^2 k^2} = \tilde{G}(k) \\ \text{with } G(x) &= \frac{1}{\sqrt{2\pi(2L\lambda^2)}} e^{-\frac{x^2}{4L\lambda^2}} \end{aligned} \right\} \quad (13)$$

This is essentially a statement of the central limit theorem. As expected, the effective lateral smoothing range from the standard deviation of the Gaussian,  $G$ , is

$$M'_2 = \lambda \sqrt{2L} \quad (14)$$

The Gaussian approximation will usually suffice, however, the exact forms of the continuous kernels,  $[S^*]^L$ , are derived in the appendix and, for  $L = 1, 2$  and  $3$ , are illustrated in Figure 1 together with their corresponding transforms.

It is simple to generalise the filters to several dimensions, but for use in the two-dimensional analyses described here the necessary filters are constructed by the successive application of the simple one-dimensional filters in the  $x$  and  $y$  directions. An important extension of the technique is obtained by permitting each filter parameter,  $\alpha$ , to vary in space, thus allowing a different amount of smoothing from one region of the field to another. Since the operators are linear it is possible to take various sums and products of them to obtain more general effective convolution functions.

### 3. ANALYSIS STRUCTURE

Having described the basic principles involved in the application of recursive smoothing filters we are now in a position to show how these filters are used in the construction of an analysis. In the notation we shall adopt, Greek suffices indicate observation position while Roman suffices denote grid points. A bracketed superfix represents the iteration index. Let  $Q_\alpha$  be each observation and the  $n$ th successive iteration of the analysis at grid point  $i$  given by  $P_i^{(n)}$ . In the absence of a background field we define  $P^{(0)} = 0$ , although in an operational setting we would of course replace zero by the background field value. The field,  $Q_i$ , is a distribution of weights derived by interpolating each weight  $Q_\alpha$  associated with an observation to the group of four surrounding grid points by bilinear interpolation.

We shall describe exactly how the weights are defined later, but in the meantime it is sufficient to note that the weights are permitted to change as the iterations proceed. In the same way we can distribute the observation residuals,  $(O_\alpha - P_\alpha^{(n)})$ , weighted by  $Q_\alpha^{(n)}$  by bilinear interpolations to get the gridpoint distribution that we symbolically denote by,

$$D^{(n)} = Q^{(n)}(O - P^{(n)}) \quad (15)$$

In the previous section we saw how recursive filters could be applied repetitively to simulate the convolution or, as in the case of spatially varying filter parameters, a 'pseudo-convolution' with a Gaussian convolution kernel. The effective standard deviation of the Gaussian is derived from the filter parameters essentially by the two-dimensional analogue of equation (14) and is denoted the 'range',  $R^{(n)}$ . Representing the associated convolution operator by  $C^{(n)}*$ , we may write the successive correction algorithm:

$$\left. \begin{aligned} P^{(0)} &= 0 \\ P^{(n)} &= P^{(n-1)} + \frac{C^{(n-1)} * D^{(n-1)}}{C^{(n-1)} * Q^{(n-1)}} \quad n > 0 \end{aligned} \right\} \quad (16)$$

At the start of the analysis the observations are each given equal weight,  $Q_\alpha^{(0)} = 1$ . The individual weights may be diminished should it appear that any observations are suspect. The field,

$$W^{(n)} = C^{(n-1)} * Q^{(n-1)} \quad (17)$$

provides a useful approximate measure of the local observation density on the scale of  $R^{(n-1)}$  and from this we may infer a characteristic distance proportional to the local standard observation separation:

$$R_w^{(n)} = \frac{1}{\sqrt{W^{(n)}}} \quad (18)$$

in units of the grid separation.

It is possible to use  $R_w$  to ensure that we do not attempt to analyse structures on a scale smaller than this. In an empirical analysis of this type it is important to attempt to fit the observations with smooth large scale fields before introducing any small scale structure, otherwise the final analysis would appear unnaturally rough. The minimum allowed scale of analysis at each iteration is a value,  $R_M$ , which is provided by the geometric series:

$$\left. \begin{aligned} R_M^{(0)} &= R_0 \\ R_M^{(n)} &= R_M^{(n-1)} S + R_L (1-S) \\ \text{ie } R_M^{(n)} &= R_L + S^n (R_0 - R_L) \end{aligned} \right\} \quad (19)$$

Then to avoid analysing detail unresolved by the observations the actual smoothing range is given by,

$$R^{(n)} = \text{Max} (R_M^{(n)}, F R_w^{(n)}) \quad (20)$$

where  $F$  is an empirical factor.

It remains to describe how the successive observation weights,  $Q_\alpha^{(n)}$ , are chosen. If we could be sure that every observation gives a faithful and representative value then they would each be given unit weight. Experience shows that occasionally an observation has an error that greatly exceeds the usual standard deviation of error, and this occurs more often than can be explained by a Gaussian error distribution. In order to ensure that these spurious observations have minimal impact on the detailed structure of the analysis the weights,  $Q_\alpha^{(n)}$ ,

are determined according to a monotonically decreasing function of  $|O_\alpha - P_\alpha^{(n)}|$ . Experiments have been conducted to try various forms and one that appears to act sensibly is

$$Q_\alpha^{(n)} = \frac{1}{1 + \left( \frac{|O_\alpha - P_\alpha^{(n)}|}{T_{ol}^{(n)}} \right)^4} \quad (21)$$

Where  $T_{ol}^{(n)}$  is an error tolerance which is made to decrease (eg exponentially) towards a fixed limit as the iteration proceeds.

Some steps towards a theoretical assessment of the analysis scheme may be taken by assuming that the observation field is sufficiently homogeneous to allow spectral methods to be used in a way that ignores effects of more than one wavenumber at a time. Thus, the approximation is not valid at scales as small as the mean observation spacing. Unlike the optimal interpolation method, which is mathematically more rigorous, the empirical successive correction method causes the analysis to approach a perfect fit with the observations (although convergence may at times be very slow).

Taking the Fourier transforms of (15) and (16) and regarding the weight field,  $Q$ , as a constant we obtained:

$$\tilde{P}_{(k)}^{(n)} = \tilde{P}_{(k)}^{(n-1)} + \frac{\tilde{C}_{(k)}^{(n-1)} (\tilde{O}_{(k)} - \tilde{P}_{(k)}^{(n-1)})}{\tilde{C}_{(0)}^{(n-1)}} \quad (22)$$

From (22) we see that the rate of convergence is dependent on wavenumber,  $k$ , with the large scale structures converging most rapidly. The ratio of residual departure from the observations before and after the nth iteration is

$$r^{(n)}(k) = \frac{\tilde{C}_{(k)}^{(n-1)}}{\tilde{C}_{(0)}^{(n-1)}} \quad (23)$$

According to this approximate analysis. The process of reducing the scale of the smoothing function,  $C$ , may be regarded as a method of increasing the rate of convergence for large  $k$  (ie small scales) since the width of the function  $\tilde{C}$  is inversely proportional to the width of  $C$  itself and both are Gaussian to a good approximation. The limitation on the extent to which we may accelerate the convergence by narrowing  $C$  comes from the non-homogeneities of the observation field which force us to use a smoothing range  $R$  slightly greater than the local observation separation in order to avoid a form of scale-aliasing.

To obtain an insight into the behaviour of the iterations in practice we show an example of successive iterations of the analysis applied to reported PMSL. The fields of successive analysis increments are shown in Figures 2-11, together with the residuals from which the increments were obtained. The final analysis is shown in Figure 12. The quality control used the formula of equation (21) with:

$$T_{ol}^{(n)} = (T_{ol}^{(o)} - T_{ol}^{(\infty)}) \sigma^n + T_{ol}^{(\infty)} \quad (24)$$

The parameters of this analysis were as follows:

Grid size:     ) East-West         : 21  
                   )                         :  
                   ) North-South     : 21

Smoothness parameter,  $L$ , of  
 equation (12)                         : 2

Filtering scales and factors

of equations (19), (20),      $R_0$  : 900 km  
    $R_L$  : 22.5 km  
    $S$  : 0.7  
    $F$  : 0.8

Quality control parameters,  $T_{ol}^{(o)}$  : 10 mb

$$T_{0\alpha}^{(\infty)} : 1 \text{ mb}$$

$$\sigma : 0.6$$

$$\text{Total number of iterations, } N : 10$$

Examples of the application of the scheme to surface wind data are illustrated in Figures 13 and 14 showing the inferred vorticity and divergence fields and the locations of individual observations. These fields are derived from the analysis of wind components by taking the appropriate fourth order spatial differences in the interior, but second order differences at the edge. Temperature and dewpoint analyses can also be routinely obtained and are exemplified in Figures 15 and 16 for a midday case. All these analyses were created without a background field and it is evident from Figure 15 that the temperatures, which are especially sensitive to the surface type, would have been better analysed from a forecast background field that contains the realistic land-sea contrasts.

A useful modification of the analysis method can be made when the variable being analysed is naturally bounded. An example would be daily rainfall amount which is never negative. In order to minimise the occurrence of spurious negative values in the analysis while preserving the smooth appearance of the field it is helpful to scale the analysed variable in a way that exaggerates its variations close to its natural limit. Taking daily rainfall as an example, we may construct pseudo-observations,  $O'_\alpha$ , derived from the actual observations,  $O_\alpha$ , according to the formula,

$$O'_\alpha = \log(O_\alpha + \delta) \tag{25}$$

where  $\delta$  is a small positive value. A scaled analysis,  $P'$ , is obtained from the set,  $\{O'_\alpha\}$ , by the standard method and the final analysis,  $P$ , is obtained by the inverse formula:

$$P = e^{P'} - \delta \quad (26)$$

An objective analysis of rainfall using a value,  $\delta = 1$  mm, is shown in Figure 17. Obviously, a similar scaling technique could be used to advantage on other variables that have either one or two natural limits.

#### 4. DISCUSSION

We have described the construction of recursive filters and demonstrated their use as the basis of a simple empirical analysis method for mesoscale domains. This method is still experimental but has already proved a useful and reasonably adaptable research tool. The scheme as described here represents the basic standard analysis method and for many applications in numerical modelling a considerable benefit could be obtained from more elaborate versions. Possible extensions that can be accommodated by the recursive filtering technique are as follows:

- a) Generalising the recursive filters (and hence the analysis scheme) to a multivariate form.
- b) Involving upper level data and smoothing increments vertically.
- c) Including data for different times and smoothing the increments temporally.
- d) Applying non-isotropic smoothing of increments in regions subject to recent flow-deformation.

Other changes that would be desirable but which would require more than a simple modification of the recursive filtering technique are:

- e) Inclusion of statistical ideas to account for observational errors.
- f) Inclusion of a balancing procedure to ensure that mass and wind fields are dynamically consistent.

Each of these changes should lead to improved analyses, although at the expense of greater complexity. It remains to be seen which changes will be justified by the associated benefits.

## REFERENCES

- Bergman, K. H. (1979) Multivariate analysis of temperatures and winds using optimum interpolation. Mon. Wea. Rev. 107 pp 1423-1443.
- Bergthorsson, P. and Döös, B. (1955) Numerical weather map analysis. Tellus 7 pp 329-340.
- Cressman, G.P. (1959) An operational objective analysis system. Mon. Wea. Rev. 87 pp 367-381.
- Gandin, L.S. (1963) Objective analysis of meteorological fields. Leningrad, Gidromet; Jerusalem, (Israel program for scientific translations. 1965 242 pp).
- Lorenc, A. (1981) A global three-dimensional multivariate statistical interpolation scheme. Mon. Wea. Rev. 109 pp 701-721.
- Rutherford, I.D. (1972) Data assimilation by statistical interpolation of forecast error fields. J. Atmos. Sci. 29 pp 809-815.

APPENDIX

Derivation of the functional form of  $[S^*]^L$

According to equation (11):

$$\tilde{S}(k) = \frac{1}{(1+i\lambda k)(1-i\lambda k)} \quad (27)$$

$$\therefore \widetilde{[S^*]^L} \equiv \tilde{S}^L(k) = \frac{1}{(1+i\lambda k)^L(1-i\lambda k)^L} \quad (28)$$

$$\therefore [S^*]^L \Big|_x = \frac{1}{2\pi} \int_{-\infty}^{\infty} \frac{e^{ikx}}{(1+i\lambda k)^L(1-i\lambda k)^L} dk \quad (29)$$

For  $x > 0$  the integration contour can be closed in the upper half plane of complex  $k$  enclosing the singularity at  $k = -\frac{1}{i\lambda}$ . Let  $k' = k + \frac{1}{i\lambda}$ .

Then:

$$[S^*]^L \Big|_x = \frac{e^{-\frac{x}{\lambda}}}{2\pi(i\lambda)^L} \int_C \frac{e^{ik'x}}{k'^L \left(1 - \frac{i\lambda k'}{2}\right)^L} dk' \quad (30)$$

where contour  $C$  encloses  $k'=0$  but not the point,  $k' = \frac{2}{i\lambda}$ .

By the calculus of residues we obtain the result:

$$[S^*]^L \Big|_x = \frac{e^{-\frac{|x|}{\lambda}}}{(2\lambda)^L i^{L-1} (L-1)!} \left. \frac{\partial^{L-1}}{\partial k'^{L-1}} \left\{ \frac{e^{ik'|x|}}{\left(1 - \frac{i\lambda k'}{2}\right)^L} \right\} \right|_{k'=0} \quad (31)$$

Using Leibnitz's theorem:

$$[S^*]^L \Big|_x = \frac{e^{-\frac{|x|}{\lambda}}}{(2\lambda)^L i^{L-1} (L-1)!} \sum_{m=0}^{L-1} \binom{L-1}{m} (i|x|)^m \left(\frac{i\lambda}{2}\right)^{L-1-m} \frac{(2L-2-m)!}{(L-1)!} \quad (32)$$

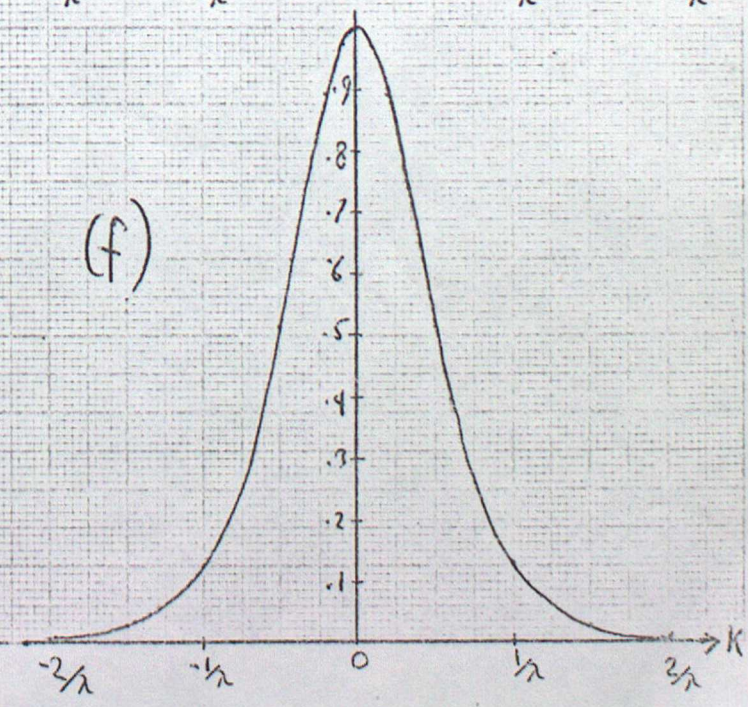
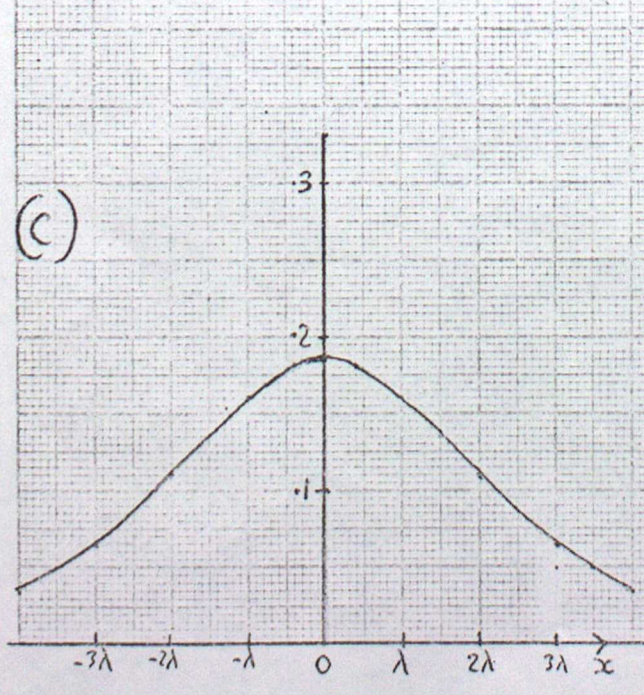
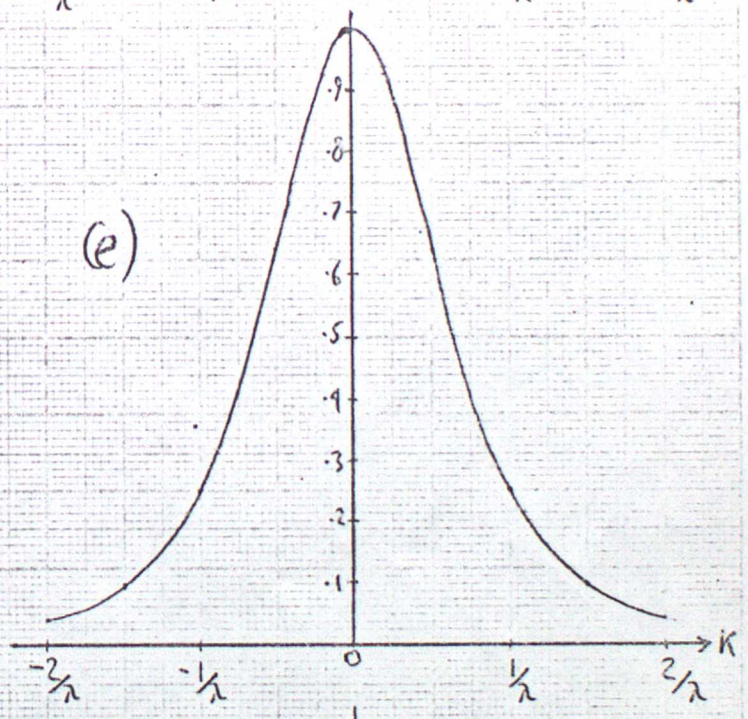
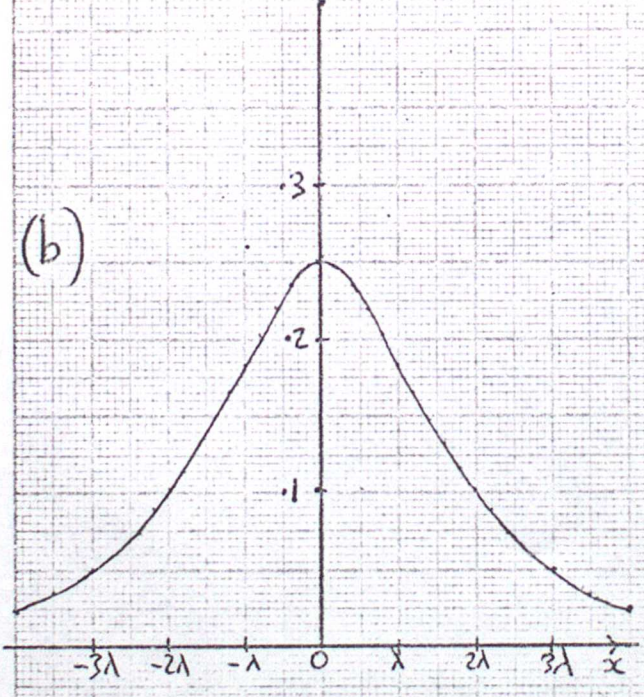
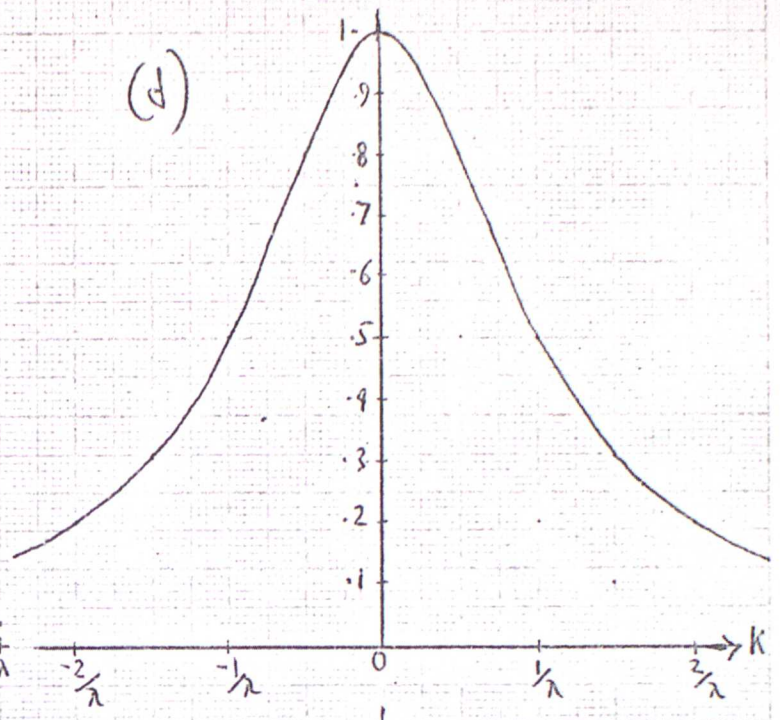
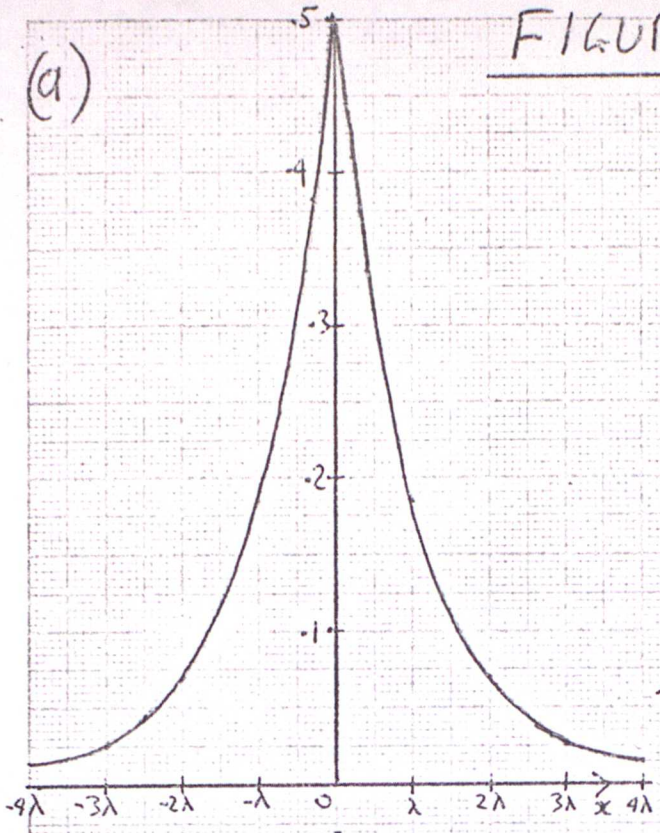
$$\text{ie } [S^*]_x^L = \frac{e^{-\frac{|x|}{\lambda}}}{2^{(2L-1)} \lambda \{(L-1)!\}^2} \sum_{m=0}^{L-1} \binom{L-1}{m} \left(\frac{|x|}{\lambda}\right)^m 2^m (2L-2-m)! \quad (33)$$

Where  $\binom{L-1}{m}$  are the usual binomial coefficients. Figure 1 shows these functions for  $L = 1, 2$  and  $3$ .

LIST OF FIGURES

- Figure 1      Kernels of the convolution operator,  $[S^*]^L$ , for  $L = 1, 2$  and  $3$  (a, b and c) and the corresponding Fourier transforms,  $\tilde{S}^L$  (d, e and f).
- Figure 2      Observations and first analysis increment (using  $TOL = 10$ ) in intervals of  $0.1$  mb corresponding to the analysis of pressure at mean-sea-level shown in Figure 12.
- Figure 3      Observation residuals and the resulting 2nd analysis increment using  $TOL = 6.4$ .
- Figure 4      Residuals and 3rd increment using  $TOL = 4.24$ .
- Figure 5      Residuals and 4th increment using  $TOL = 2.94$ .
- Figure 6      Residuals and 5th increment using  $TOL = 2.17$ .
- Figure 7      Residuals and 6th increment using  $TOL = 1.70$ .
- Figure 8      Residuals and 7th increment using  $TOL = 1.42$ .
- Figure 9      Residuals and 8th increment using  $TOL = 1.25$ .
- Figure 10     Residuals and 9th increment using  $TOL = 1.15$ .
- Figure 11     Residuals and 10th increment using  $TOL = 1.09$ .
- Figure 12     Analysis of PMSL for 127 2.6.81 in millibars, composed by the accumulation of successive corrections shown in Figures 2-11.
- Figure 13     Vorticities from a surface wind analysis for 127 2.6.81 in units of  $10^{-5} s^{-1}$ .
- Figure 14     Divergences from a surface wind analysis for 127 7.6.81 in units of  $10^{-5} s^{-1}$ .
- Figure 15     Analysed screen temperatures in units of  $1^\circ C$  for 127 2.6.81.
- Figure 16     Analysed dewpoints in  $^\circ C$  for 127 2.6.81.
- Figure 17     Detailed analysis of daily rainfall for the period between 09Z 5.6.80 and 09Z 6.6.80.

# FIGURE 1



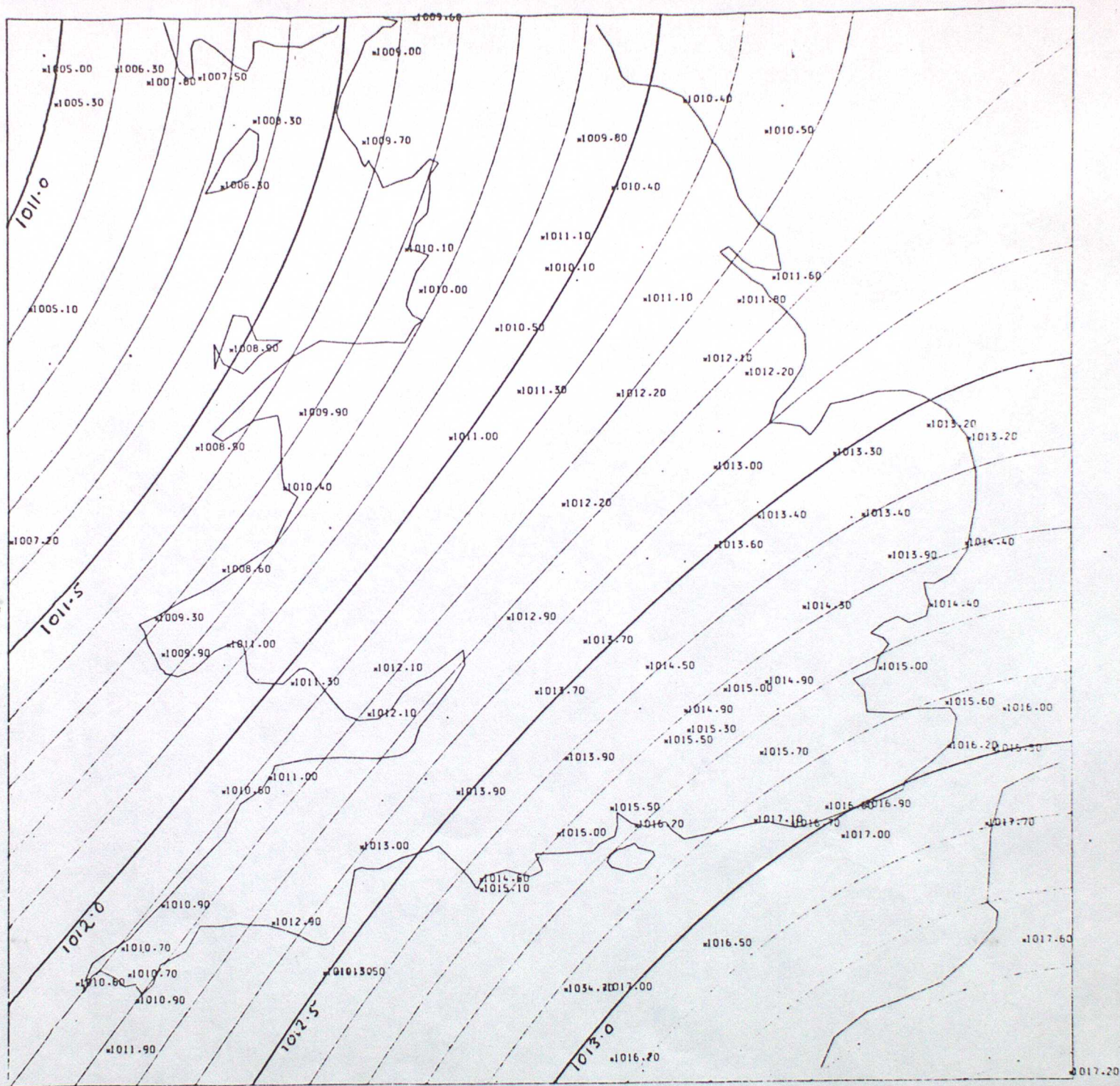


FIGURE 2

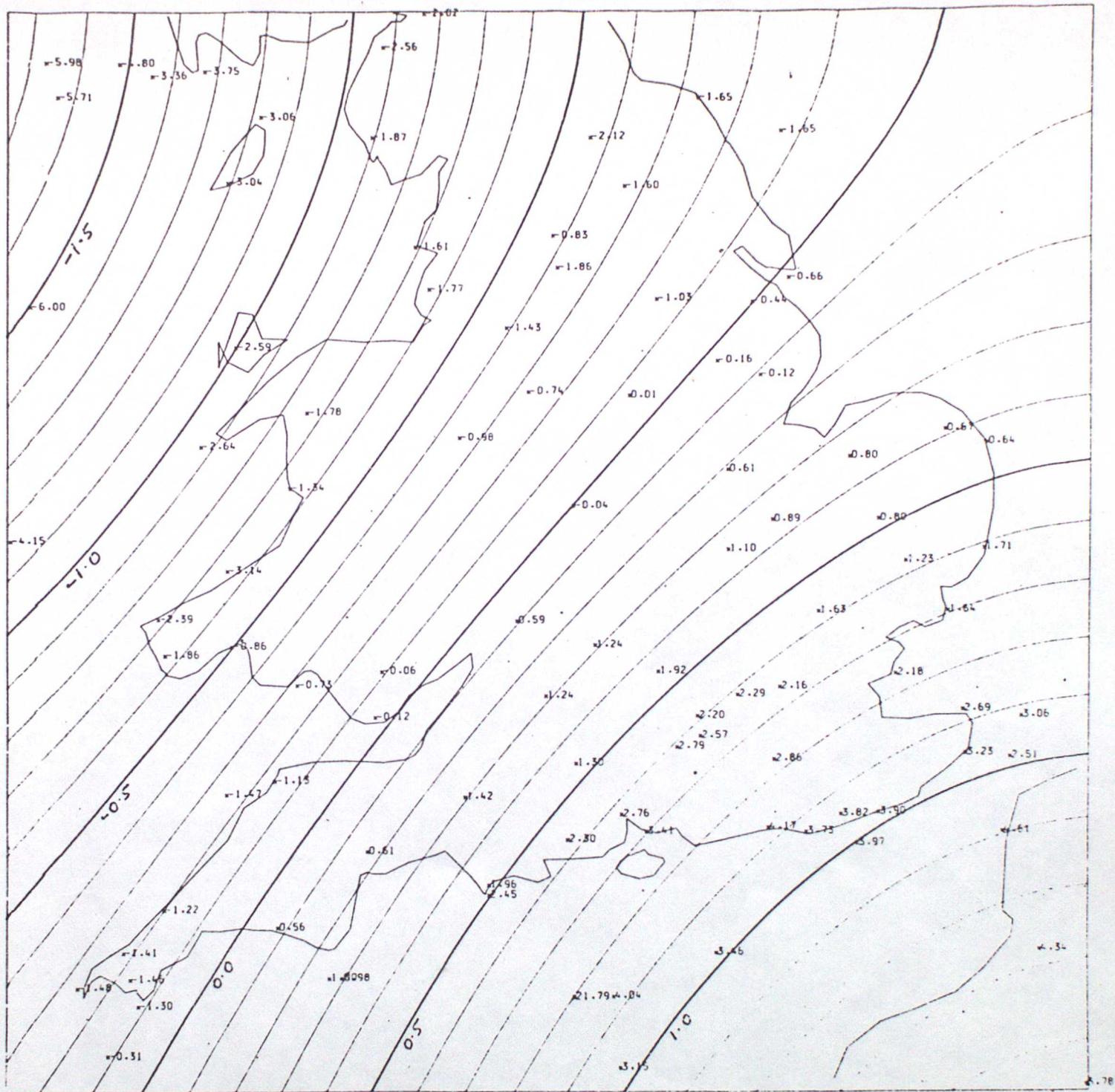


FIGURE 3







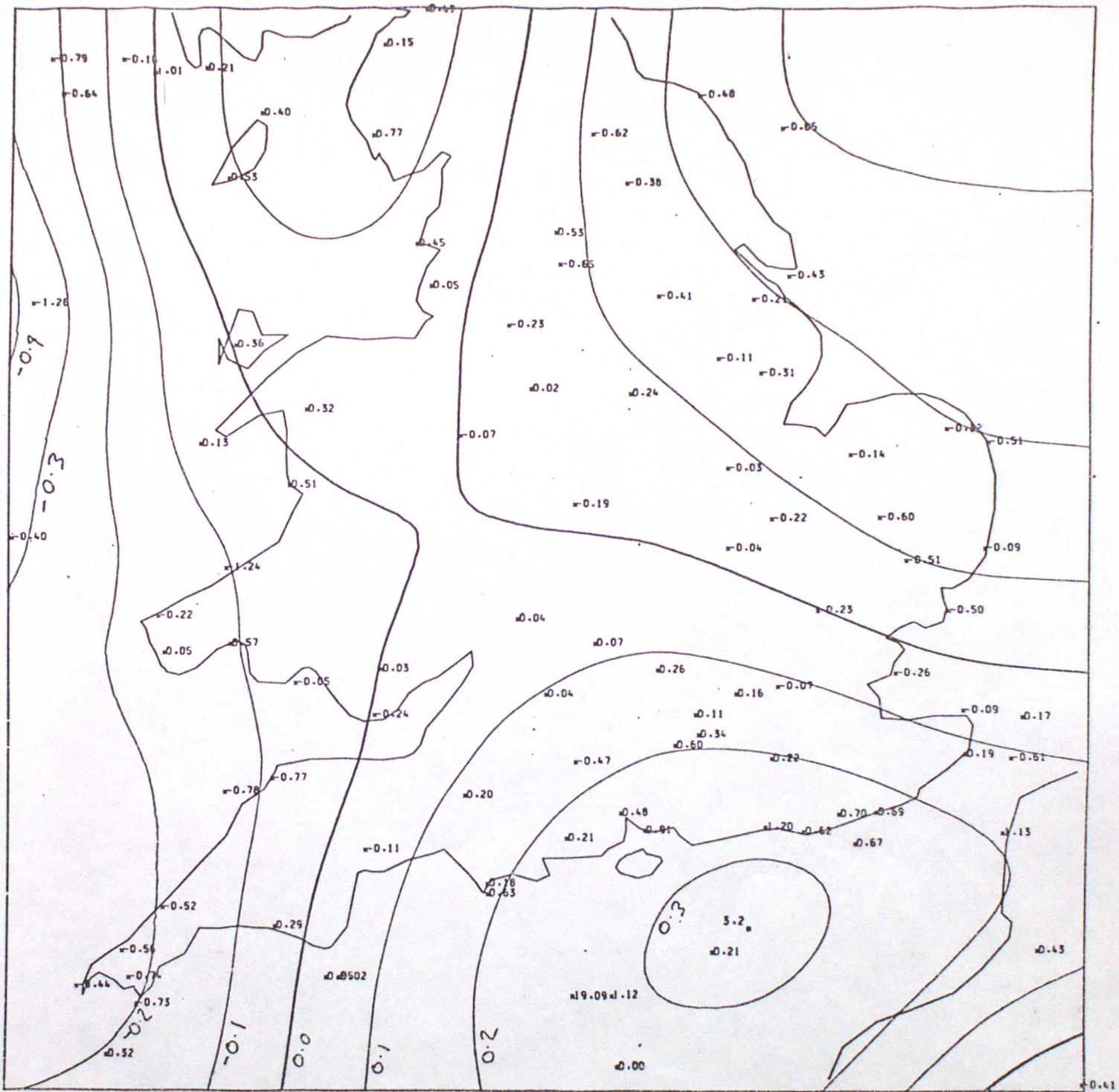


FIGURE 7



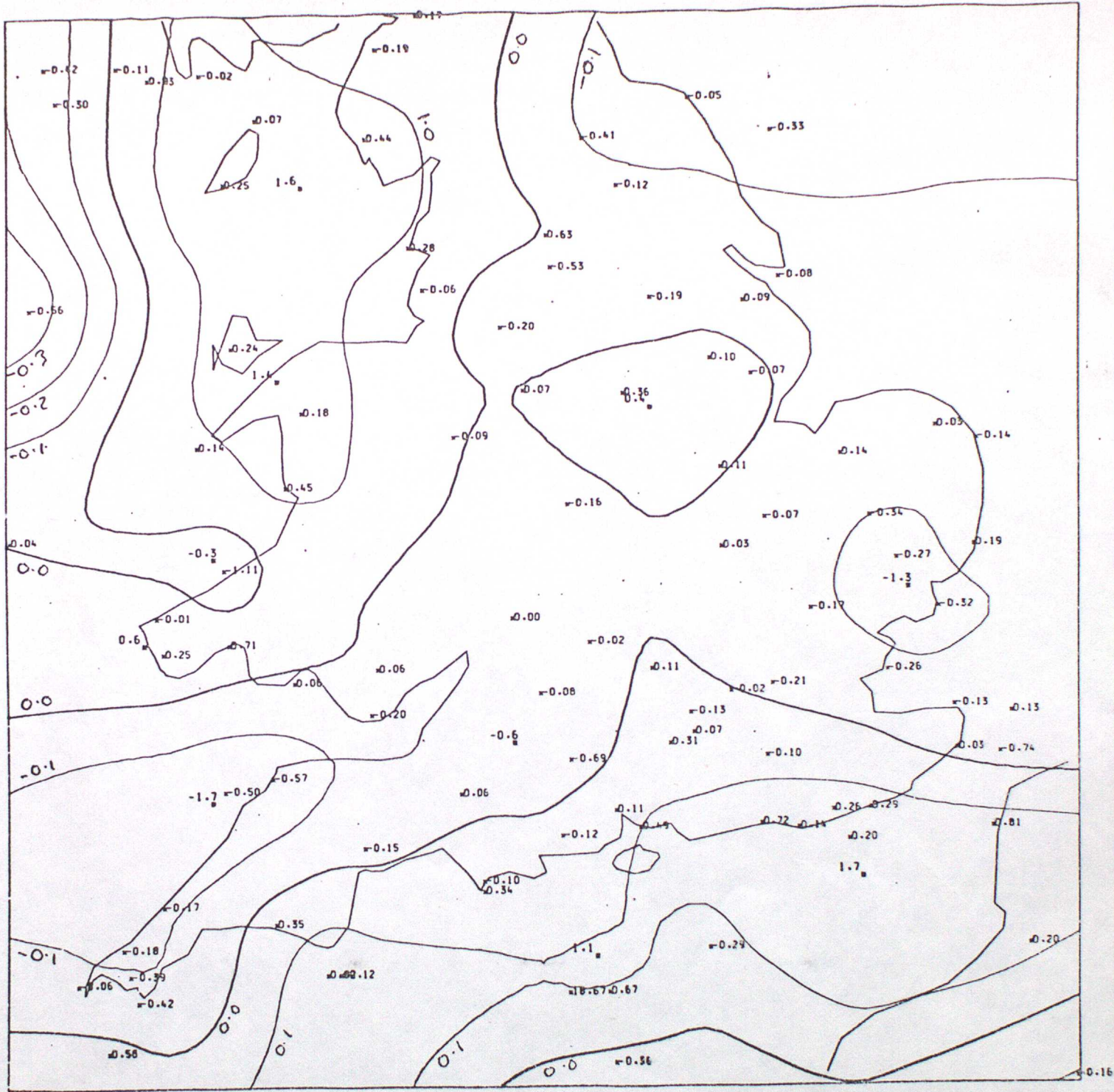


FIGURE 9

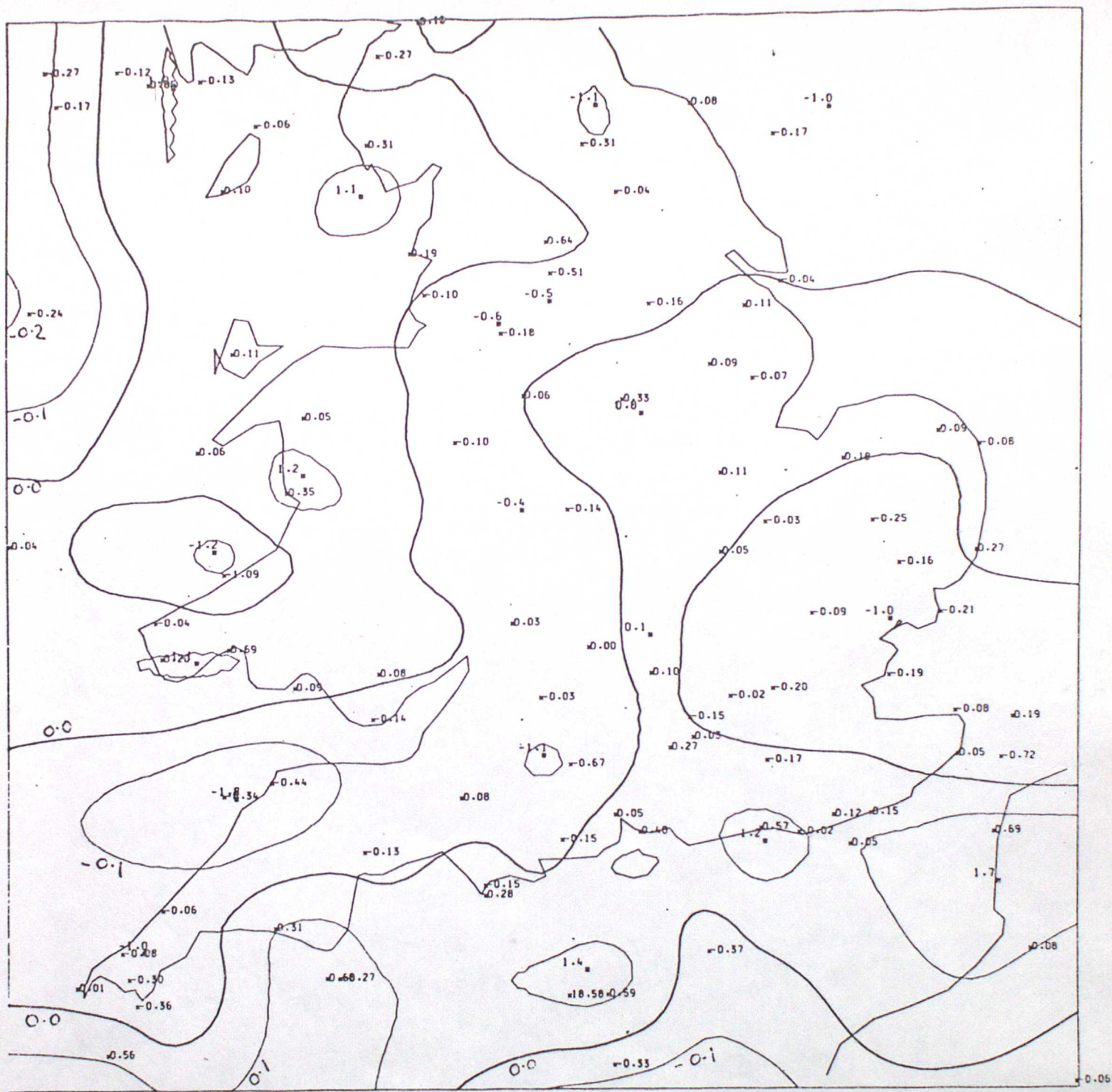


FIGURE 10



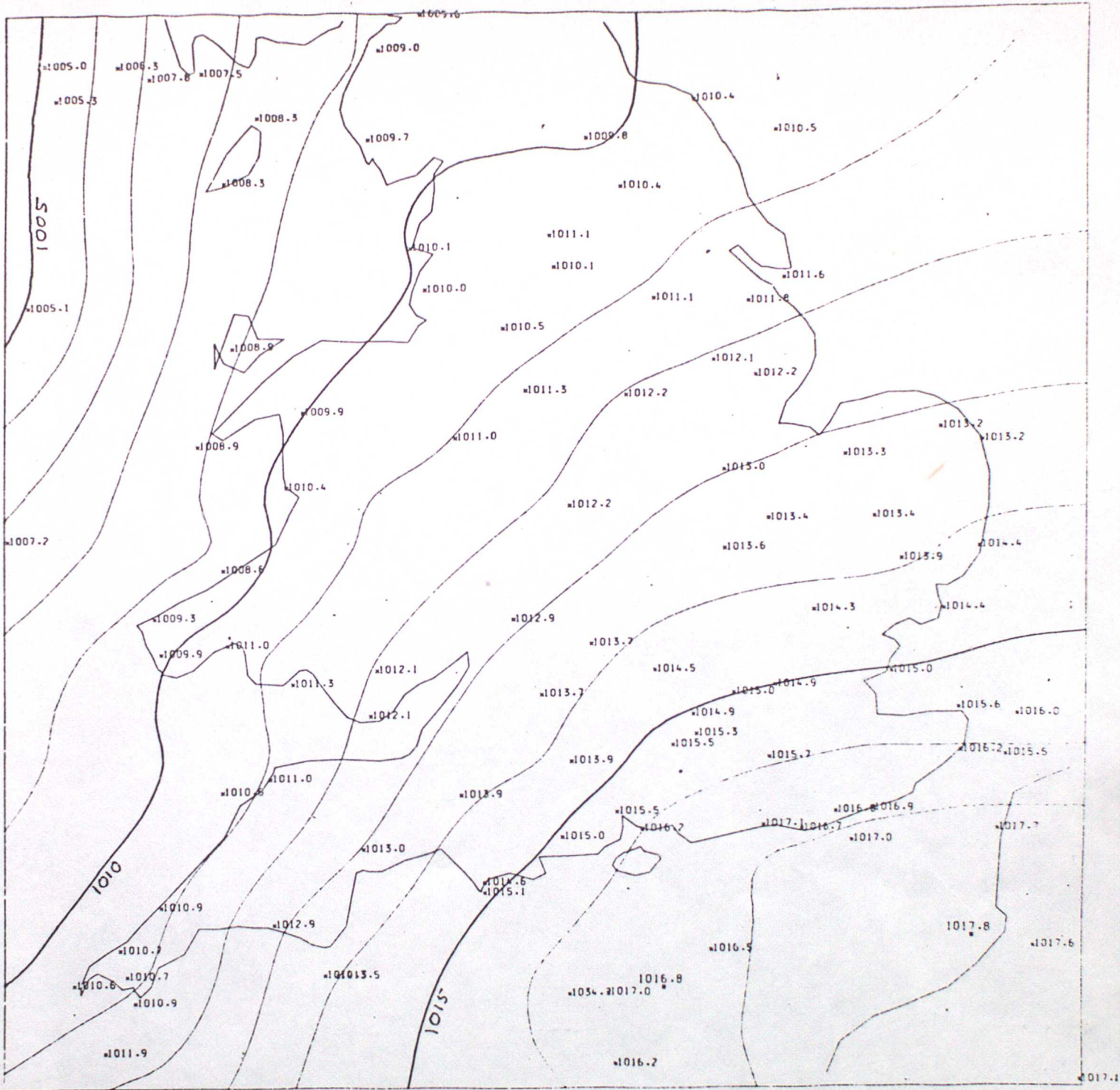


FIGURE 12

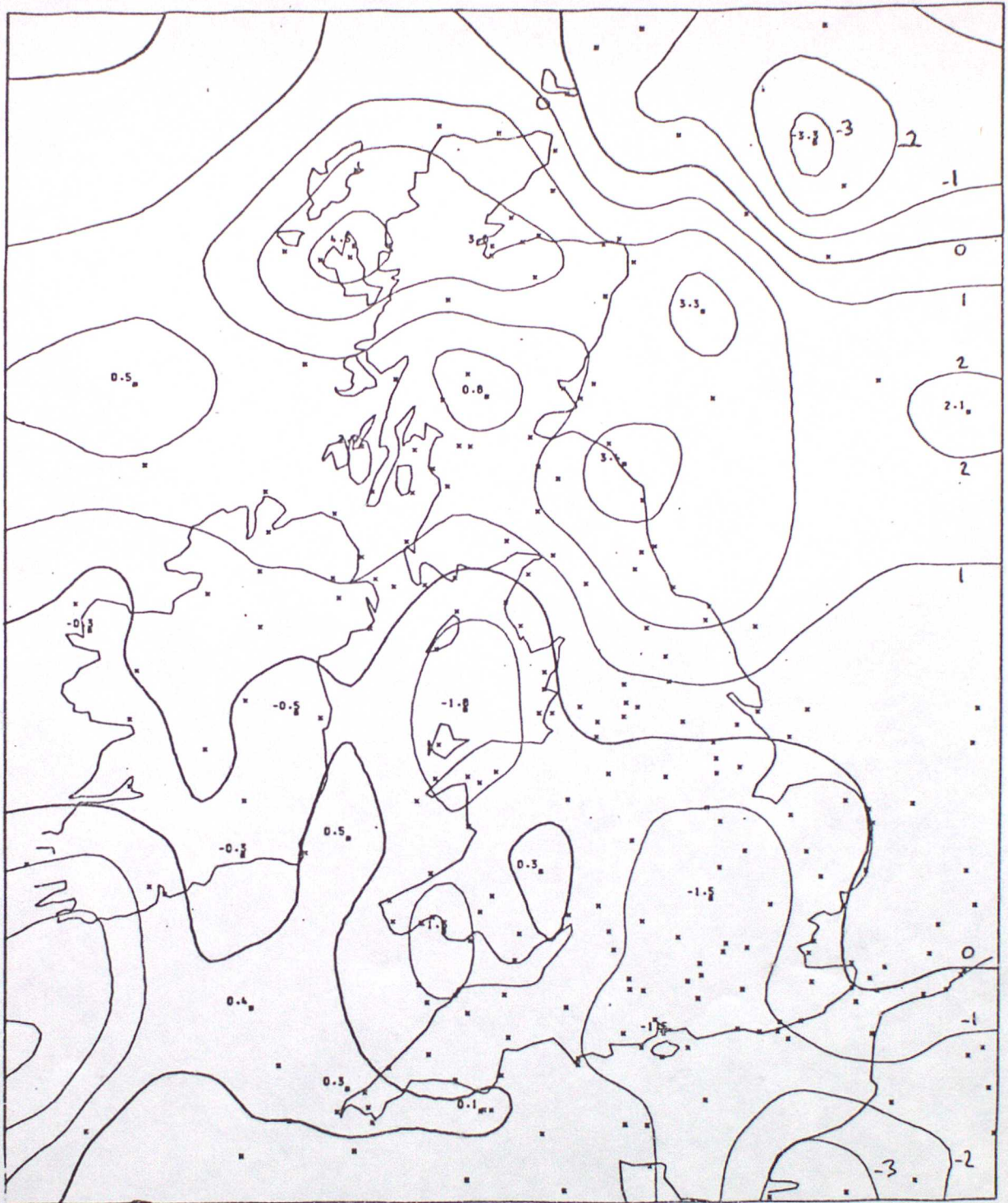


FIGURE 13



FIGURE 14

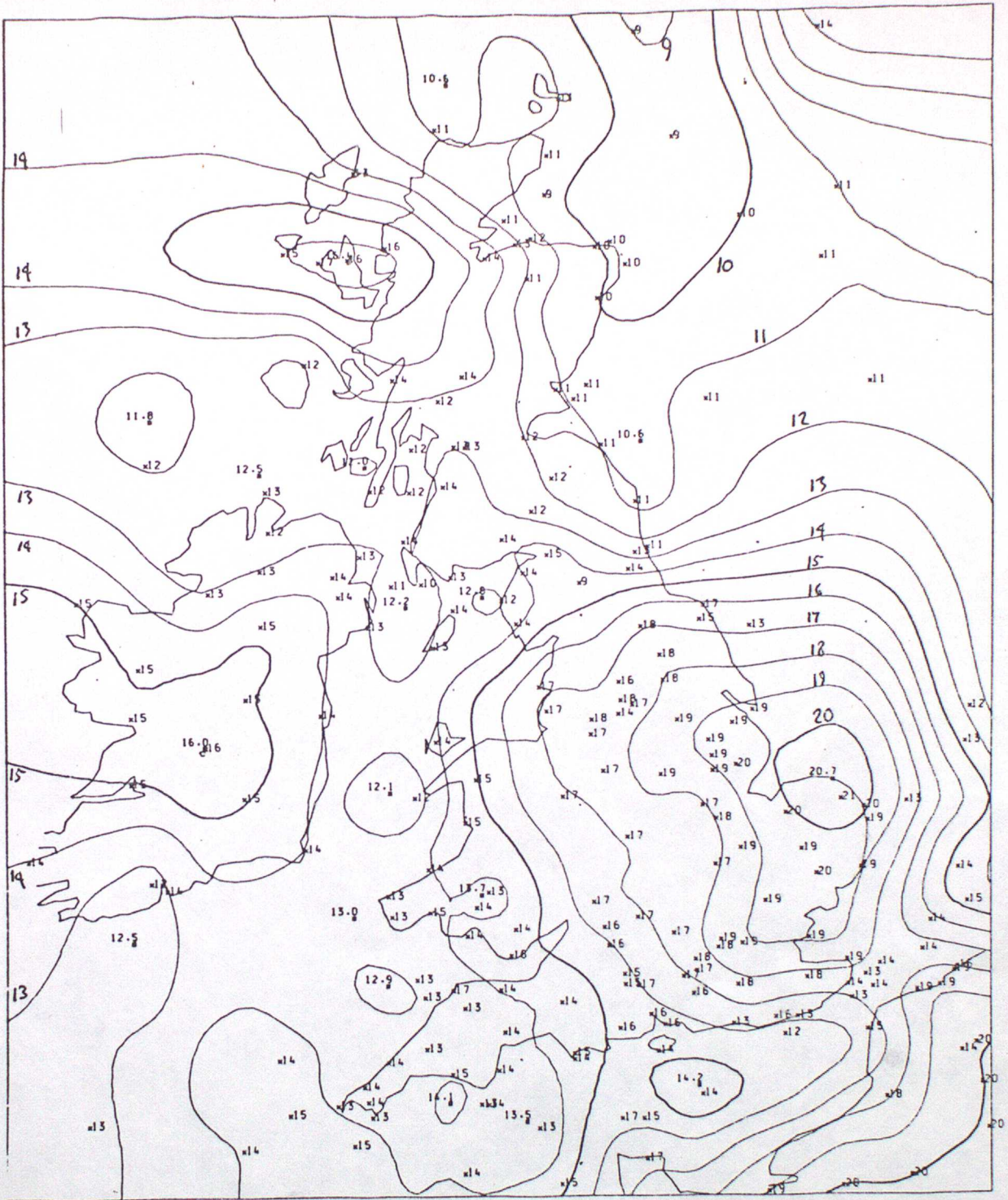


FIGURE 15

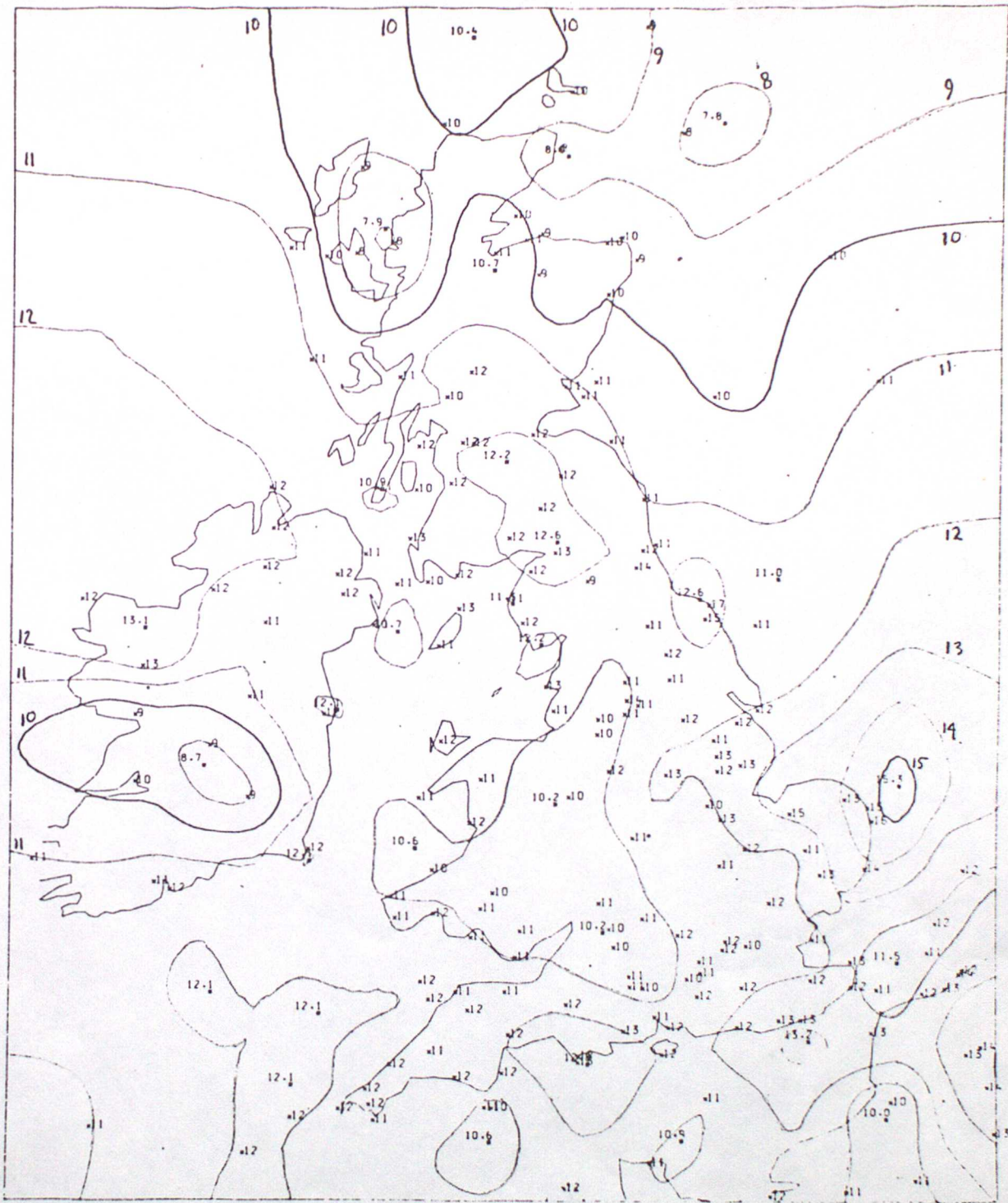


FIGURE 16

# FIGURE 17

MINIMUM CONTOUR 1 mm  
CONTOUR INTERVAL 5 mm

